Feasibility study of autofluorescence mammary ductoscopy

Alexandre Douplik
Ontario Cancer Institute
University Health Network
7-417 610 University Avenue
Toronto, M5G 2M9 Canada
and
Xillix Ltd.
620 University Avenue
Toronto, Ontario M5G 2C1 Canada
and
Friedrich-Alexander Universität Erlangen-Nürnberg
Erlangen Graduate School in Advanced Optical Technologies
Paul-Gordan-Straße 6
Erlangen, 91052, Germany

Wey L. Leong
Alexandra M. Easson
University Health Network
Princess Margaret Hospital
Department of Surgical Oncology
610 University Avenue, Suite 3-130
Toronto, M5G 2M9 Canada
and
Ontario Cancer Institute
University Health Network
7-417 610 University Avenue
Toronto, M5G 2M9 Canada

Susan Done
George Netchev
Ontario Cancer Institute
University Health Network
7-417 610 University Avenue
Toronto, M5G 2M Canada

Brian C. Wilson
Ontario Cancer Institute
University Health Network
7-417 610 University Avenue
Toronto, M5G 2M9 Canada
and
University of Toronto
Department of Medical Biophysics
Ontario Cancer Institute, Princess Margaret Hospital
610 University Avenue, Room 7-411
Toronto, M5G 2M9 Canada

Abstract. We report the technical feasibility of autofluorescence ductoscopy in the *ex-vivo* setting. The current imaging algorithm for visualizing tumor tissue against the normal tissue background, although developed and optimized for other organs, appears to provide discrimination between intraductal tumor and normal ductal tissue. Point fluoroscopy is also performed. Although the optical "geometry" for this is different, the findings are consistent with the imaging observations. © *2009 Society of Photo-Optical Instrumentation Engineers.* [DOI: 10.1117/1.3210773]

Keywords: ductoscopy; cancer; autofluorescence; imaging; spectroscopy.

Paper 09131R received Apr. 9, 2009; revised manuscript received Jun. 25, 2009; accepted for publication Jun. 26, 2009; published online Aug. 25, 2009.

1 Introduction

Mammary ductoscopy (MD)[1] uses a submillimeter endoscope inserted into breast ducts for direct visualization and to yield high-resolution white-light images of the ductal epithelium. Clinically, it has been most commonly used in the management of pathological nipple discharge (PND), as it allows removal of intraductal papilloma therapeutically and guidance of surgical excision intraoperatively.[2] MD has also been used as a diagnostic tool for ductal carcinoma, which is the most common form of cancer in the breast. Here, we sought to enhance the diagnostic accuracy of MD by the addition of autofluorescence imaging, and diffuse reflectance and fluorescence point spectroscopy. In this exploratory study, we added these capabilities into a commercial ductoscope and used the

Address all correspondence to: Alexandre Douplik, Erlangen Graduate School in Advanced Optical Technologies (SAOT), Friedrich-Alexander Universität Erlangen-Nürnberg, Paul-Gordan-Straße 6, Erlangen, Germany, 91052. Tel: +49-9131-8525879; E-mail: alexandre.douplik@aot.uni-erlangen.de

1083-3668/2009/14(4)/044036/6/$25.00 © 2009 SPIE

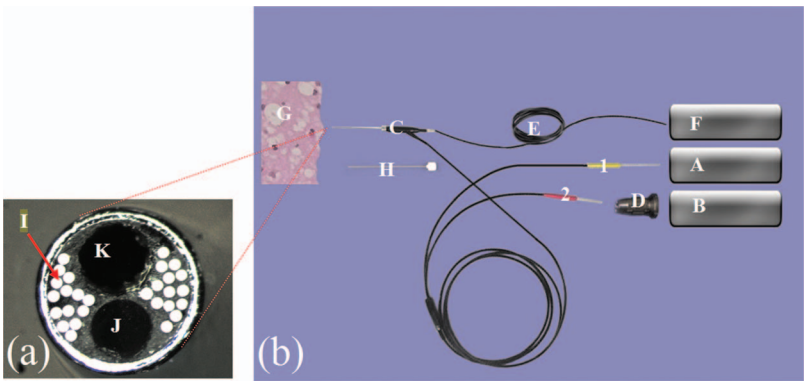

Fig. 1 Experimental setup for autofluorescence and white-light imaging, and for diffuse reflectance and fluorescence point spectroscopies. (a) Close-up of the distal tip of the ductoscope. (b) Schematic of the imaging/spectroscopy elements: A is an endoscopic light source comprising a 200-mW high-pressure mercury arc lamp (VIP R 150/P24 qN2, Osram, Germany); B shows the image capture and processing unit, comprising a standard three-color CCD camera for white-light imaging and an intensified CCD camera for autofluorescence imaging; C show the ductosope (Fibertec, Japan), including the light guide (1) and 3000 fiber imaging bundle (2): D is the eyepiece for universal mounting; E is the collection fiber for diffuse reflectance spectroscopy (150-μm core silica, NA=0.22, Thorlabs,); F is the combined reflectance and fluorescence spectroscopy unit, including collimating lenses (f/2.7: Edmund Optics, Barrington, New Jersey), automated filter wheel (AB-300, Spectral Products, Putnam, Connecticut), and spectrometer (MSL-CS1-USB-VR®, Medspeclab Incorporation, Canada); G is tissue (duct wall); H is the biopsy probe; I shows the light delivery fibers; J is the imaging guide (with 0.35-mm-diam coupled lenses); and K is the biopsy channel (0.3 mm diam in the 0.7-mm scope).

system to examine ten fresh mastectomy specimens from patients with known ductal carcinoma.

Besides assessing the technical feasibility of autofluorescence to produce acceptable image quality in the ducts, we also assessed whether there are distinct changes in the tissue autofluorescence images between malignant and benign tissues that potentially can facilitate visualization of lesions that are not seen under conventional white-light dusctoscopy. We used blue-light excitation and detected the green fluorescence emission, as has been reported in other hollow organs such as the gastrointestinal tract,[3] bronchus,[4] and urinary bladder.[5] Collagen and elastin are believed to be the main fluorophors responsible for the autofluorescence in the green range under blue excitation.[6] The question remains as to what is the true source of the autofluorescent contrast between malignant and normal/benign tissues that makes such lesions visible under fluorescence examination, but not visible under conventional white-light examination:[7] modification of the intrinsic autofluorescent properties of the tissue, or alterations of tissue absorption and/or scattering, for example, due to the cancer angiogenesis, or both? We recognize, of course, that frank tumor as examined here does not necessarily have the same optical characteristics as premalignant lesions. For simplicity, we used an existing autofluorescence imaging system that had been developed and optimized for lung and GI endoscopy. *A priori*, this is not necessarily optimal for ductoscopy, so we included the point fluorescence and reflectance spectroscopies to gain further data that may inform the interpretation of the imaging results and, potentially, to provide additional information that may be used to optimize the imaging parameters for this specific application.

2 Materials and Methods

Ten consented patients with a preoperative diagnosis of palpable invasive ductal carcinoma who required a mastectomy were recruited into the study between May 2005 and July 2008. This *ex-vivo* pilot study was approved by the Research Ethics Board at University Health Network, Toronto. All mastectomy specimens were examined within 1 to 1.5 h after resection. The mastectomy specimen was placed onto a dome-shaped pad to spread the milk ducts for easier passage of the rigid fiber ductoscope (model MS-611, Fibertech, Japan). Two different ductoscopes were used. The first three cases were carried out with a 1.1-mm external diameter instrument. However, this was found to limit access, so that the remaining seven cases were done using a 0.7-mm ductoscope. Both devices had a working length of 70 mm, field of view of 70 ± 5 deg, and depth of view of 1 to 10 mm.

As shown in Fig. 1, the ductoscope was coupled via a standard eyepiece to a fluorescence endoscopic imaging system (OncoLIFE®, Xillix Technologies Corporation, British Columbia, Canada, now Pinpoint®, Novadaq Technologies Corporation, Ontario, Canada). The principle of operation (Fig. 2) and technical details have been reported elsewhere.[7,8] Briefly, standard white-light and autofluorescence images are recorded at 30 frames per second using 6.3-mW broadband light and 5.3-mW blue band (390 to 450 nm), respectively. The operator can switch between the two modes of imaging rapidly. In fluorescence imaging mode, the endogenous fluorescence (collected within 490 to 580 nm) is normalized by the red reflectance (690 to 750 nm) to minimize effects due to varying tissue distance and angle or shadowing. In general for other organs, premalignant tissues have a reduced green autofluorescence relative to normal tissues when excited by blue light, such that normal tissue appears as cyan, while abnormal tissue is shown as a range of red color in each pixel, depending on the red-to-green ratio. The central 16×12 pixels are averaged over four frames and continuously displayed on the fluorescence image as a numerical color value (NCV). The higher the NCV, the lower the fluorescence intensity, which has been associated with neoplasia: hence high NCVs helped to confirm the abnormality seen on the fluorescence image, as shown in Figs. 3(b) and 3(d). The deviation of the NCVs found across the investigated area

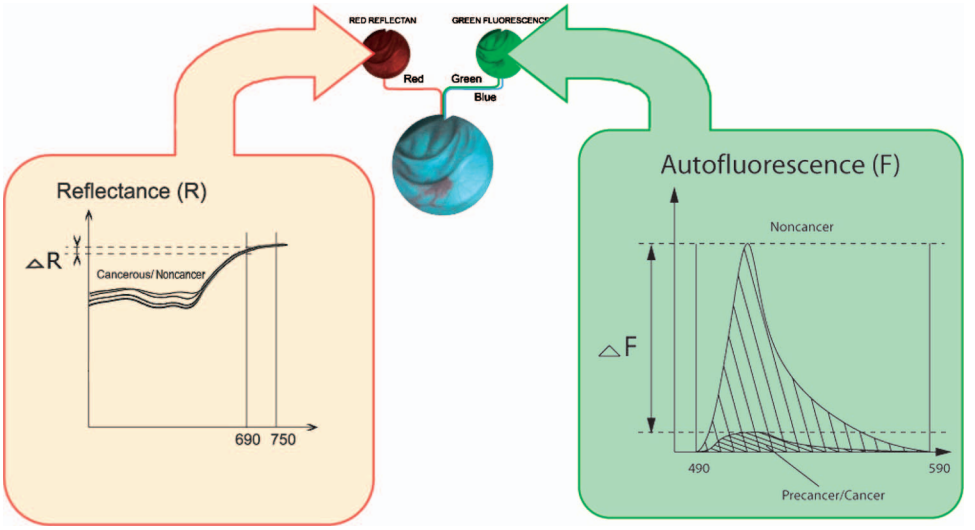

Fig. 2 Principle of the autofluorescence imaging system. An autofluorescence image is formed from two separate images: in each pixel the green fluorescence signal F (490 to 580 nm) collected by the ICCD camera is normalized by the red reflectance signal R (690 to 750 nm) collected by the standard three-color CCD camera. The numerical color values (NCVs) are displayed on a false-color image, which generally shows high levels of NCV as reddish and low levels as blue-green.

(within a single spot of observation) was ±15% for normal tissue and ±25% for cancerous tissue.

The point spectroscopy system comprised a small-diameter silica fiber coupled to a fiber optic spectrometer through an automated filter wheel. The light delivered by the fiber scope was used for illumination/excitation. The collecting fiber was placed through the biopsy channel and positioned in the center of the imaging field of view, gently touching the tissue surface. Two different filters were used: a color correction filter (C-filter, Edmund Optics, Barrington, New Jersey), that balanced the blue and red components of the diffuse reflectance spectrum to be within the detector dynamic range, and a customized filter (YF2: Barr Associates, Westford, Massachusetts) that enabled the green fluorescence to be collected with high efficiency (transmission 90% at 455 to 575 nm), together with a fraction of the diffuse blue and red reflectance (steep cut-off from 90 to 1% transmission between 455 and 445 nm and from 90 to 5 % between 575 and 590 nm). The combination of YF2 with the existing OncoLIFE® excitation light source filter almost completely blocks (OD=6) the excitation light within the green band, so that only the autofluo-

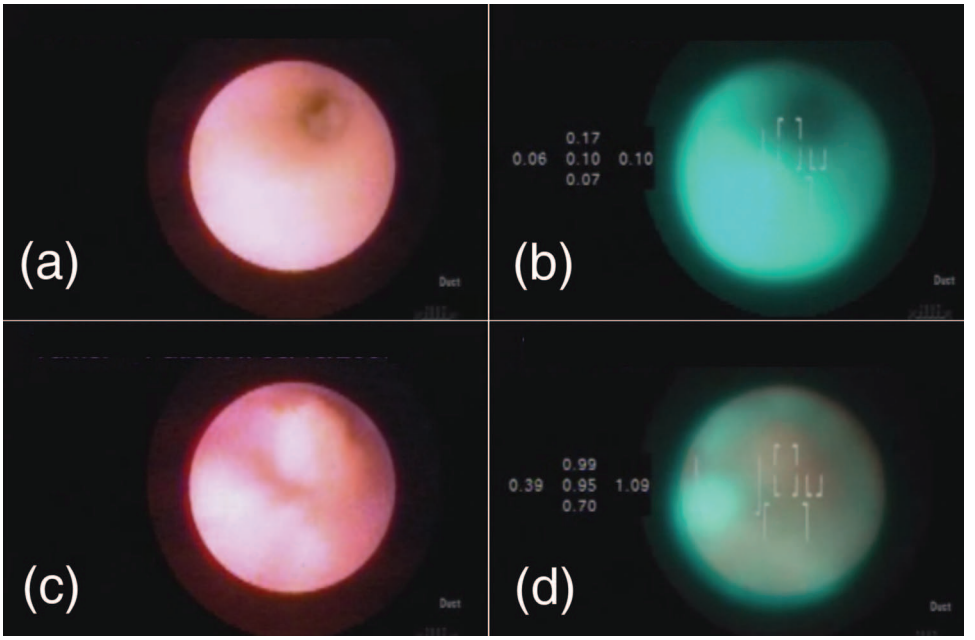

Fig. 3 Case 2 (valid): normal region [(a) white light and (b) autofluorescence] compared to tumor region [(c) white light and (d) autofluorescence]. The forward-looking field of view is approximately 1 mm. The NCV locations and corresponding values are seen in (b) and (d).

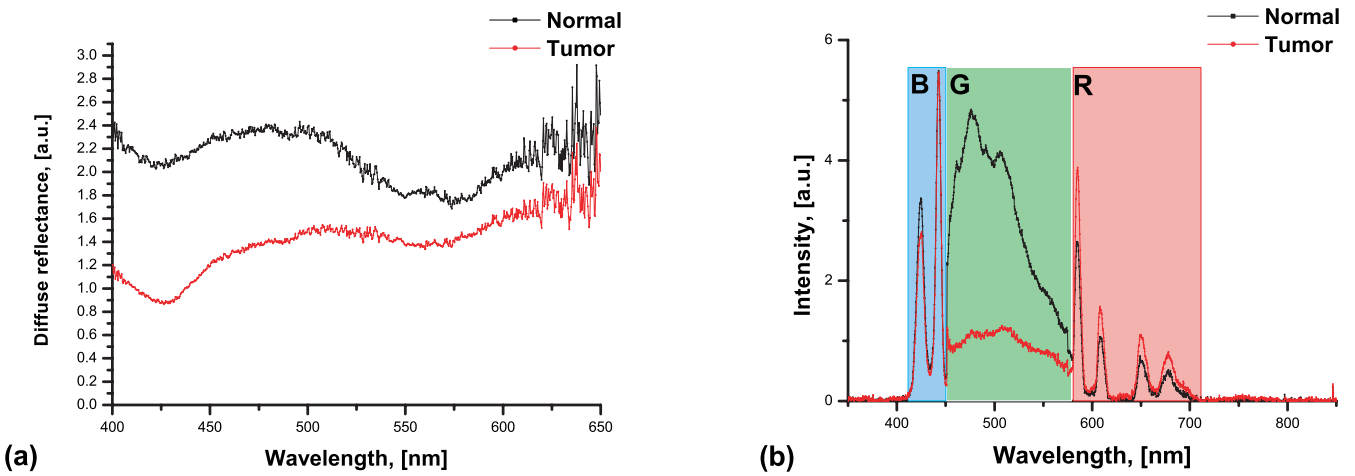

Fig. 4 Case 9: (a) diffuse reflectance spectra over regions of normal and tumor tissue, (b) autofluorescence spectra in the green band G, also providing acquisition of some portions of blue (B-band) and red (R-band) reflectance from the excitation light. The sharp peaks within the blue (B) and red (R) bands are mercury lines from the arc lamp source.

rescence is collected [G-band in Fig. 4(b)], while also providing acquisition of some portions of blue and red reflectance from the excitation light [B- and R-bands accordingly on Fig. 4(b)], whose intensities are comparable with the that of the autofluorescence. This permits simultaneous acquisition of all three parameters (blue reflectance, green autofluorescence, and red reflectance) in a single spectrum within the detector dynamic range [Fig. 4(b)]. The spectra were collected using customized software driving the filter wheel and the OncoLIFE® light source to switch at 2.5 Hz between the diffuse reflectance and fluorescence modes, and integrating 10 to 15 spectra in each mode at each observation spot. The integrated fluorescence signal had a standard deviation at a given site of typically $\pm 8\%$ for normal tissue and 15% for cancerous lesions.

The procedure for each mastectomy specimen was first to perform white-light ductoscopy. Once a region of tumor was identified, the white-light image video was collected for 10 to 15 s, and then the imaging system was switched to fluorescence mode for another 15 to 20 s. Following this, point spectra were collected for both diffuse reflectance and fluorescence, for typically 10 to 15 spectra each, sequentially under software control. The diffuse reflectance data were processed according to the method of Ref. 9 to determine the blood oxygenation rate (SO2, %) and relative total blood volume fraction (THb, a.u.). The total data acquisition in each region of interest took about 4 to 5 min. In the first five valid cases, the imaging and spectroscopy were performed over two to three regions of both tumor and normal tissue to assess the reproducibility of the measurements. In the remaining cases, only a single area of each tissue type was examined. In each area, once the optical interrogation was completed (white light and fluorescence imaging, diffuse reflectance and fluorescence spectra), a special biopsy needle with a side window at the tip was used to obtain specimens of tumor and adjacent normal tissue (similar to that described in Ref. 10).

3 Results and Discussion

In total we examined ten mastectomy specimens with histologically confirmed malignant tumor: three with the 1.1-mm ductoscope and seven with 0.7-mm ductoscope, the latter providing high-quality videos and spectra data. A detailed analysis and discussion of the clinical findings will be presented in a subsequent paper.

Ductoscopy can access ducts about 6 to10 cm from the nipple openings. Smaller ducts can also be cannulated when distended with saline. It cannot reach ducts that are less than about 0.7 mm when distended, even though the natural diameter before distension can be very small. We typically see fourth and fifth duct bifurcations. This being said, most ductal carcinomas and papillomas that produce nipple discharge are likely to be within reach of ductoscopy. Peripheral lesions are unlikely to have nipple discharge. Our judgement is that $>95\%$ of breast cancers and papilloma with nipple discharge can be seen.

Figure 3 shows examples of ductoscopic images, in both white-light and autofluorescence modes, from a 53-year-old woman who underwent a modified radical mastectomy for a 3.5-cm invasive ductal carcinoma (AJCC T2N1M0). A corresponding video clip is also available.

As shown in Fig. 3 and Video 1, the images had adequate brightness and resolution in both imaging modes. Figures 3(a) and 3(b) show images taken from a normal duct from the same patient in white-light and fluorescence modes, respectively. In white-light mode, the intraductal carcinoma appeared as irregular protrusions into the ductal lumen, with color similar to the surrounding ductal tissue [Fig 3(c)]. In fluorescence mode [Fig 3(d)], the same intraductal carcinoma appeared reddish compared to the surrounding ductal tissue, which was blue-green (cyan) in color. It was noted that debris seen in the lumen of the normal duct [Fig 3(a)], which can be misinterpreted as cancer, appropriately appeared blue-green in fluorescence mode, demonstrating the ability of fluorescence ductoscopy to differentiate cancer from noncancer tissue in this case.

Figure 4 shows an example of the reflectance and autofluorescence spectra. The point spectroscopy and imaging gave qualitatively similar results. However, the tumor-to-normal tissue contrast is better represented in the imaging mode (NCV=1:10 versus 1:5). This is, in part, due to the imaging

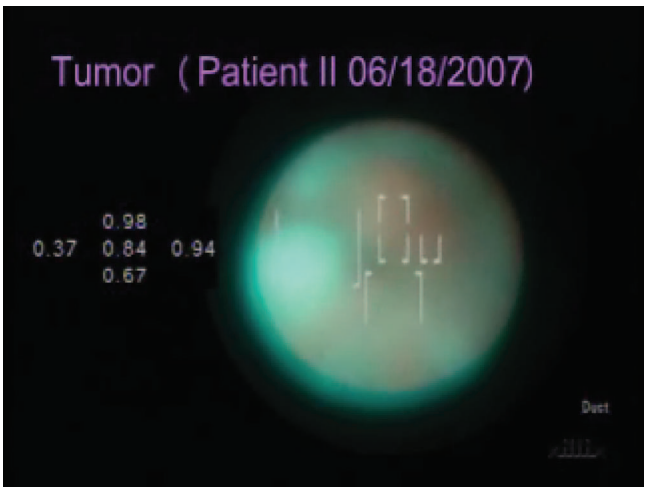

Video 1 Video recording during ductoscopy of a mastectomy specimen from a 53-year-old woman who underwent a modified radical mastectomy for a 3.5-cm invasive ductal carcinoma (AJCC T2N1M0). Figure 3 shows corresponding still images. The clip starts in autoflorescence mode in a region of normal duct, which appears blue-green (cyan) in color. In the subsequent white-light mode, the normal duct appears reddish and smooth. Debris seen in the lumen of the normal duct appears blue-green in autofluorescence mode. In the second half of the video clip, ductal carcinoma appears red with a high NCV value in autoflorescence mode, while the corresponding tumor in white-light mode appears reddish in color similar to that of normal ductal epithelium except for the irregular surface. (QuickTime, 4.7 MB). [URL: http://dx.doi.org/10.1117/1.3210773.1]

and spectroscopy bands not being identical, but also probably indicates that there is a difference in the effective sampling depth in the tissue between the wide-field imaging and localized point spectroscopy techniques, as has been reported in other studies.[11] The fluorescence spectra could be normalized by either the blue or red reflectance, and the former appeared to provide more consistent discrimination between normal and cancerous tissue.

The normalized fluorescence spectra showed reduced integrated intensity (450 to 580 nm) in tumor compared with normal ductal epithelium, except in one case. Hence, the existing imaging algorithm developed for lung and GI autofluorescence endoscopy appears to be potentially valid also for MD. Blood oxygenation (SO_2) and relative total volume fraction (THb) retrieved from the diffuse reflectance spectra showed considerably higher SO_2 (30 to 35 versus 2 to 5% accordingly) and lower THb (28 to 35 versus 52 to 60 a.u.) in normal tissue versus malignancy. This difference, particularly in terms of THb, can partly help to explain the autofluorescence contrast observed *ex vivo*, due to the higher absorption of the excitation light and higher reabsorption of the autofluorescence emission by hemoglobin in malignant tissues.

Whether or not it is necessary or possible to fine tune the algorithm specifically for ductoscopy will require a larger cohort of patients and should be done *in vivo* to be maximally relevant to the ultimate clinical implementation. In particular, it may be important that the blood flow and tissue architecture are maintained, since these could affect particularly the reflectance spectra, and this is supported by the fact that the patient-to-patient fluorescence spectra (prior to normalization) were more consistent than the diffuse reflectance spectra.

It is important to reiterate that this work was performed on patents with frank tumor, whereas the ultimate major clinical impact will be in patients with early-stage lesions. Hence, it may be necessary to reoptimize the imaging parameters in the next phase of the work, although the current parameters are already optimal for early-stage disease in other hollow organs such as the bronchus and GI tract, so that it may not be necessary to make major changes. Regardless, we are encouraged at least by the technical feasibility of the approach, the assessment of which was the primary objective in the present study. Based on clinical experience with conventional ductoscopy, we anticipate that it will actually be easier to perform these studies *in vivo*, since the ducts tend to collapse in the mastectomy specimens, making access more difficult.

4 Conclusions

We demonstrate the technical feasibility of autofluorescence ductoscopy, even in the more challenging *ex-vivo* setting. The current imaging algorithm for visualizing tumor tissue against the normal tissue background, although developed and optimized for other organs, appears to provide discrimination between intraductal tumor and normal ductal tissue. The point spectroscopies appear to be consistent with the imaging findings, and to demonstrate any other particular spectral bands that should be employed, at least over the wavelength ranges used and for frank malignancy. The next step will be to carry out similar studies *in vivo* and in patients who do not have known malignancy, e.g., women presenting with abnormal nipple discharge. More detailed analysis of the clinical findings and implications of the present study will be reported separately.

Acknowledgments

This study was supported by the Ontario Research and Development Challenge Fund, the Princess Margaret Hospital Foundation, and Xillix Technologies Corporation, Canada. The authors thank B. Shnapir of Barr Associates and S. Miike of Fibertech, Japan, for their cooperation.

References

1. B. Pereira and K. Mokbel, "Mammary ductoscopy: past, present, and future," *Int. J. Clin. Oncol.* **10**, 112–116 (2005).
2. V. R. Jacobs, S. Paepke, H. Schaaf, B. C. Weber, and M. Kiechle-Bahat, "Autofluorescence ductoscopy: a new imaging technique for intraductal breast endoscopy," *Clin. Breast Cancer* **7**, 619–623 (2007).
3. J. Haringsma, W. Prawirodirjdo, and G. N. J. Tytgat, "Accuracy of fluorescence imaging of dysplasia in Barrett's esophagus," *Gastroenterologist* **116**, A 418 (1999).
4. K. Haussinger, H. Becker, F. Stanzel, A. Kreuzer, B. Schmidt, J. Strausz, S. Cavaliere, F. Herth, M. Kohlhaufl, K. M. Muller, R. M. Huber, U. Pichlmeier, and C. T. Bolliger, "Autofluorescence bronchoscopy with white light bronchoscopy compared with white light bronchoscopy alone for the detection of precancerous lesions: a European randomised controlled multicentre trial," *Thorax* **60**, 496–503 (2005).
5. W. Zheng, W. Lau, C. Cheng, K. C. Soo, and M. Olivo, "Optimal excitation-emission wavelengths for autofluorescence diagnosis of bladder tumors," *Int. J. Cancer* **104**, 477–481 (2003).
6. J. Qu, C. MacAulay, S. Lam, and B. Palcic, "Laser-induced fluorescence spectroscopy at endoscopy: tissue optics, Monte Carlo modeling and *in vivo* measurements," *Opt. Eng.* **34**(11), 3334–3343 (1995).
7. A. Douplik, S. Zanati, N. Marcon, M. Cirocco, B. Wilson, J. Boehm, S. Rychel, and J. Fengler, "Combined autofluorescence and white-light endoscopy for improved detection of dysplastic colonic le-

sions," in *Biomed. Opt. OSA Tech. Digest*, paper ME6 (2006).
8. M. J. Simoff, "Autofluorescence in the detection of lung cancer," in *Thoracic Endoscopy: Advances in Interventional Pulmonology*, M. J. Simoff, D. H. Sterman, and A. Ernst, Eds., pp. 1–20, Blackwell Publishing (2006).
9. A. Stratonnikov and V. Loschenov, "Evaluation of blood oxygen saturation in vivo from diffuse reflectance spectra," *J. Biomed. Opt.* **6**(4), 457–467 (2001).
10. M. Hünerbein, M. Raubach, B. Gebauer, W. Schneider, and P. Schlag, "Ductoscopy and intraductal vacuum assisted biopsy in women with pathologic nipple discharge," *Breast Cancer Res. Treat.* **99**, 301–307 (2006).
11. R. S. DaCosta, B. C. Wilson, and N. E. Marcon, "Spectroscopy and fluorescence in esophageal diseases," *Best Prac. Res. Clin. Gastroenterol.* **20**(1), 41–57 (2006).